Research
A SCIENCE PARTNER JOURNAL

RESEARCH ARTICLE

Mechanoluminescent Materials Enable Mechanochemically Controlled Atom Transfer Radical Polymerization and Polymer Mechanotransduction

Zexuan Li[1†], Zhenhua Wang[1*†], Chen Wang[1], Wenxi Li[2], Wenru Fan[1], Ruoqing Zhao[1], Haoyang Feng[1], Dengfeng Peng[3*], and Wei Huang[1*]

[1]Frontiers Science Center for Flexible Electronics, Institute of Flexible Electronics, Northwestern Polytechnical University, Xi'an 710072, China. [2]School of Materials Science and Engineering, Northwestern Polytechnical University, Xi'an 710072, China. [3]Key Laboratory of Optoelectronic Devices and Systems of Ministry of Education and Guangdong Province, College of Physics and Optoelectronic Engineering, Shenzhen University, Shenzhen 518060, China.

*Address correspondence to: iamwhuang@nwpu.edu.cn (W.H.); iamzhwang@nwpu.edu.cn (Z.W.); pengdengfeng@szu.edu.cn (D.P.)
†These authors contributed equally to this work.

Citation: Li Z, Wang Z, Wang C, Li W, Fan W, Zhao R, Feng H, Peng D, Huang W. Mechanoluminescent Materials Enable Mechanochemically Controlled Atom Transfer Radical Polymerization and Polymer Mechanotransduction. *Research* 2023;6:Article 0243. https://doi.org/10.34133/research.0243

Submitted 29 May 2023
Accepted 13 September 2023
Published 3 October 2023

Copyright © 2023 Zexuan Li et al. Exclusive licensee Science and Technology Review Publishing House. No claim to original U.S. Government Works. Distributed under a Creative Commons Attribution License 4.0 (CC BY 4.0).

Organic mechanophores have been widely adopted for polymer mechanotransduction. However, most examples of polymer mechanotransduction inevitably experience macromolecular chain rupture, and few of them mimic mussel's mechanochemical regeneration, a mechanically mediated process from functional units to functional materials in a controlled manner. In this paper, inorganic mechanoluminescent (ML) materials composed of CaZnOS-ZnS-SrZnOS: Mn^{2+} were used as a mechanotransducer since it features both piezoelectricity and mechanolunimescence. The utilization of ML materials in polymerization enables both mechanochemically controlled radical polymerization and the synthesis of ML polymer composites. This procedure features a mechanochemically controlled manner for the design and synthesis of diverse mechanoresponsive polymer composites.

Introduction

Polymer mechanotransduction has emerged to convert the input mechanical energy into productive chemical or light signals among synthetic polymers [1–6]. Normally, force-responsive groups (mechanophores) are inserted into polymer chains to undergo a mechanochemical reaction when exposed to external force [7–14], giving rise to mechanochromism, mechanoluminescence, mechanocatalysis, etc [15–25]. Although elegant designs have been increasingly developed in the past decade, most examples of polymers containing mechanophore inevitably experience bond rupture [26–32], and few of them mimic mussel's mechanochemical regeneration, a mechanically mediated process from monomer to biopolymer in a controlled manner [33–34].

Recently, as an alternative mechanotransducer to mechanophore in synthetic polymers, piezoelectric materials have gained increasingly interest for mechanically controlled radical polymerizations including atom transfer radical polymerization (ATRP) and reversible addition fragmentation chain transfer polymerization [35–54]. These methodologies have been demonstrated to synthesize well-defined polymers with predicted molecular weight, high chain-end fidelity, and narrow molecular distribution [55]. Taking advantage of this chemistry, Esser-Kahn and colleagues [56–58] developed a series of mechanochemically strengthened composites comprising synthetic thiol-based polymers and piezoelectric nanoparticles, which would be cross-linked to ultrasonic agitation or mechanical vibration. Although these mechanochemically formed polymer networks could be recovered into linear polymer chains under reduction, they can hardly be used for the repeatable mechanoresponsive process because thiols are not stable and highly reactive to oxidation [59–61].

Semiconductor heterojunction, combined with its piezoelectric and semiconductive properties, has done a lot of original work in moderating elastic mechanoluminescence [62–66]. In this study, ternary-heterojunction ML CaZnOS-ZnS-SrZnOS: Mn^{2+} was designed as a mechanotransducer to conduct mechanically controlled ATRP (mechano-ATRP) for the synthesis of repeatably responsive mechanoluminescent (ML) composites. ML materials were synthesized by high-temperature solid-phase reactions, and their luminescence properties were reported in previous work [65]. ML materials were used in this work because it has 2 functions: piezoelectricity and mechanoluminescence. The utilization of piezoelectricity facilitates electron transfer under mechanical forces to convert the deactivators (Cu^{II}/L) into the activators (Cu^{I}/L), thus activating polymerization to

synthesize desired polymers in a controlled manner (Fig. 1). In addition, the resultant polymer composites containing ML powders possess the ability to emit orange luminescence upon force. This procedure enables the synthesis of various ML composites with well-defined polymers, tunable compositions, and mechanical performance.

Results

In a preliminary experiment, mechano-ATRP of methyl acrylate (MA) was attempted by using ML materials as the mechanotransducer for the mechanoelectrical reduction of Cu (II) to Cu (I). A Schlenk flask was charged with 200/1/0.03/0.12 molar ratio of MA, ethyl α-bromoisobutyrate (EBiB) (initiator), $CuBr_2$/TPMA (catalyst), dimethyl sulfoxide (DMSO), and ML materials under nitrogen (N_2). The mixture was then subjected to ultrasonic irradiation at 45 kHz. As shown in (Table), the conversion of polymerization approached 92% after 6-h ultrasonic agitation under identical conditions, yielding polymethyl acrylate (PMA) with $M_n = 10{,}100$ and $Đ = 1.07$ (entry 2). While the ultrasound (US) was replaced by ultraviolet (UV) irradiation, the polymerization could not proceed (entry 1), indicating the advantage of the US over UV light toward the control of the heterogeneous polymerization process.

To further validate the role of ML materials in polymerization, the effect of ML loadings on mechano-ATRP was investigated. As shown in Fig. 2, all the reactions revealed an induction period, indicating a slow activation in the beginning. This is different from the previous piezoelectric systems (ZnO, $BaTiO_3$), potentially because of the lower surface area for the microscale ML materials compared to the nanoscale piezoelectric particles. The polymerization reached only 9% conversion in the absence of ML materials after 5 h of ultrasonic irradiation (Fig. S2). When the loading of ML materials increased to 2.4 wt%, the polymerization gave 54% conversion after 5 h of ultrasonic irradiation, giving a PMA with $M_n = 9{,}500$ and $Đ = 1.12$ (Figs. S3 and S5). The conversion increased to 77% with 4.8-wt% loading of ML materials, affording

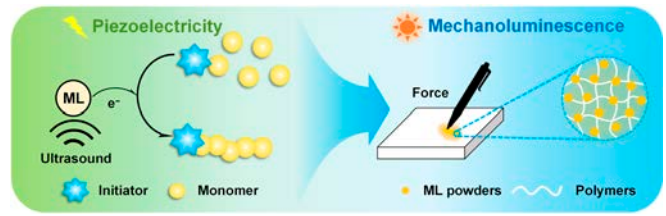


Fig. 1. Dual roles of ML materials.

a polymer with $M_n = 13{,}800$ and $Đ = 1.08$ (Fig. S4). These results showed that ML materials are essential to the mechanically controlled activation and elevation of polymerization.

To examine whether this procedure can be used to synthesize polymers with predicted molecular weight, mechano-ATRP of MA targeting various degrees of polymerization (DP_T) was conducted. EBiB and $CuBr_2$/TPMA changed depending on the target DP_T. As shown in Table, when DP_T was set at 200, the conversion of MA reached 92%, giving a PMA with $M_n = 10{,}100$ and $Đ = 1.07$ after 6 h of US irradiation (entry 2).

Mechano-ATRP with $DP_T = 400$ attained 87% conversion, giving a PMA with $M_n = 24{,}900$ and $Đ = 1.09$ (entry 3). The polymerization reaction targeting $DP_T = 800$ achieved 78% conversion, affording PMA with $M_n = 39{,}300$ and $Đ = 1.12$ (entry 4). Mechano-ATRP of methyl methacrylate (MMA) with $DP_T = 200$ gave 64% conversion, producing polymethyl methacrylate (PMMA) homopolymer with $M_n = 16{,}300$ and $Đ = 1.29$ after 10 h of ultrasonic irradiation (entry 5). The conversion of polymerization targeting $DP_T = 400$ reached 56%, giving well-defined PMMA with $M_n = 18{,}600$ and $Đ = 1.29$ (entry 6). When DP_T was set at 800, the conversion approached 37%, yielding PMMA with $M_n = 28{,}200$ and $Đ = 1.31$ (entry 7).

Furthermore, this procedure was expanded into the polymerization of other monomers including butyl acrylate (BA), butyl methacrylate (BMA), 2-methoxyethyl methacrylate (MEMA), and ethyl acrylate (EA) in Table. All monomers were successfully polymerized to give well-defined polymers under ultrasonic

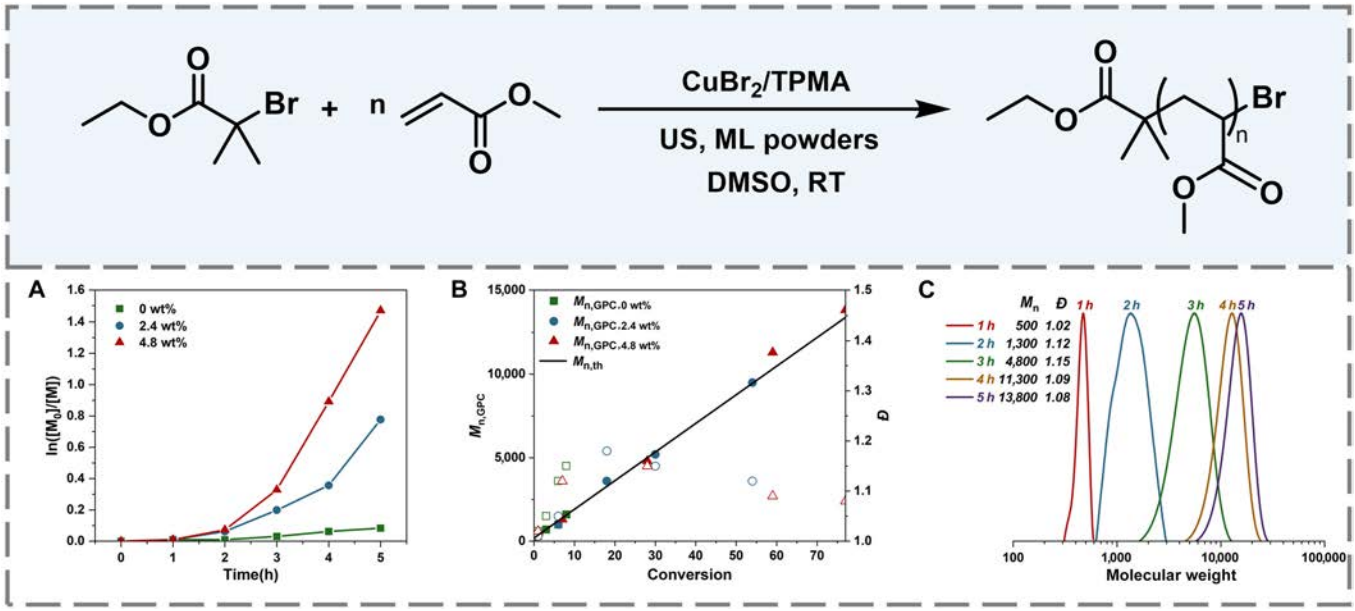


Fig. 2. (A) Kinetics of mechano-ATRP with different ML materials (red: 0 wt%; green: 2.4 wt%; blue: 4.8 wt%). (B) The number-average molecular weight and dispersity $Đ$. (C) GPC traces of polymers. Reaction conditions: $[MA]_0/[CuBr_2]_0/[TPMA]_0/[EBiB]_0 = 200/0.03/0.12/1$, 50% (v/v) DMSO, 25 °C, 45 kHz, 300 W.

Table. Mechano-ATRP for the synthesis of homopoly(meth)acrylates with different DP_T

Entry [a]	Monomer	DP_T	T (h)	ML (wt%)	Conversion [b]	$M_{n,th}$ [c]	$M_{n,GPC}$ [d]	$Đ$ [d]
1 [e]	MA	200	6	4.8	7%	1,400	600	1.24
2	MA	200	6	4.8	92%	16,000	10,100	1.07
3	MA	400	6	4.8	87%	30,100	24,900	1.09
4	MA	800	6	4.8	78%	53,800	39,300	1.21
5	MMA	200	10	4.8	61%	12,400	14,200	1.23
6	MMA	400	10	4.8	48%	19,300	14,700	1.26
7	MMA	800	10	4.8	37%	29,800	28,200	1.31
8 [f]	BA	200	4	4.8	68%	17,800	14,800	1.15
9 [f]	MEMA	200	4	4.8	50%	14,600	15,400	1.19
10	EA	200	4	4.8	64%	13,000	12,400	1.10
11 [g]	BMA	200	6	4.8	38%	10,900	15,400	1.33

[a]Reaction conditions: $[Monomer]_0/[CuBr_2]_0/[TPMA]_0/[EBiB]_0 = X/0.03/0.12/1$ (X = 200, 400, or 800), 4.8 wt% ML powders, 50% (v/v) DMSO, 25 °C, 45 kHz, 300 W.

[b]Conversion was determined using ^{1}H NMR.

[c]Calculated based on conversion (i.e., $M_{n,th} = M_{EBiB} + [Monomer]_0/[EBiB]_0 \times conversion \times M_{monomer}$).

[d]Determined by GPC in THF, based on linear PMMA as the calibration standard.

[e]The polymerization was conducted in UV light (365 nm).

[f]The polymerization was conducted in DMF.

[g]The polymerization was conducted in mixed solvents (DMF/anisole = 1/1).

irradiation. The experimental molecular weight of all the synthesized polymers matched well with the theoretical value accompanied with narrow molecular weight distribution.

To confirm the retention of chain-end functionality in the mechano-ATRP procedure, chain extension reaction was carried out. The first block was conducted under the standard conditions, yielding a PMA-Br macroinitiator with $M_n = 4{,}000$ and $Đ = 1.15$ at 23% conversion. The chain extension of PMA-Br with EA was further conducted. After 4 h of ultrasonic bath, the chain-extended polymerization of PMA-*b*-PEA-Br was prepared with $M_n = 8{,}400$ and $Đ = 1.05$ as shown in Fig. S20. To further examine the chain-end retention, matrix-assisted laser desorption/ionization-time of flight (MALDI-TOF) mass spectrometry was used. The spectrum showed a steady increase in molecular mass as shown in Fig. S21, which is consistent with the molecular weight of MA unit ($M_n = 86$). The strongest peak revealed a molecular weight of 8,271 which matched well with the corresponding gel permeation chromatography (GPC) trace ($M_n = 8{,}700$). Another distribution at 8,255 can be attributed to the removal of a methyl group by laser irradiation [67–68]. In conclusion, the MALDI-TOF spectra confirmed the high chain-end fidelity of PMA synthesized via this mechano-ATRP procedure.

To examine the temporal control over polymerization, ultrasonic agitation was switched on/off for several cycles. Samples were periodically withdrawn from the vessel and analyzed by GPC to monitor the evolution of polymer M_n over time and analyzed by ^{1}H nuclear magnetic resonance (NMR) spectroscopy to calculate monomer conversion (Fig. S22). As shown in Fig. 3, the growth of polymer molecular chains can be well controlled by ultrasonic irradiation. The molecular weight of the polymer produced a remarkable increase under US, whereas during the US-off periods negligible monomer conversion was observed (Fig. 3A and B). Excellent control over mechano-ATRP of MMA throughout this US on/off cycle, and the experimental molecular weight of the polymer is slightly higher than the theoretical value ($M_n = 8{,}700$, $M_{n,th} = 6{,}300$), potentially because of the low initiation efficiency of EBiB for MMA (Fig. 3C and D).

To study the ML properties, a series of polymer composites with different glass transition temperatures (T_g) were synthesized via the standard mechano-ATRP procedure (Fig. 4C to E). T_g of the ML composites increased from 16 to 100 °C when the monomer changed from MA to MMA. All the composites emitted yellow light upon force repeatably. The emission peak of the ML spectrum was located at 600 nm (Fig. S26). A camcorder was employed to capture the luminescence induced by the sliding object and intercept photographs of the ML materials producing the mechanoluminescence trajectory. When combined and superimposed together, the photos yielded an overall trajectory of 3 complete letters "IFE" in Fig. 4B. In addition, the thermal properties of the ML polymer composites were further investigated by thermogravimetric analysis (Fig. S28). The decomposition temperature (T_d) corresponding to 5% weight loss of the composites varied from 270 °C (PMMA) to 360 °C (PMA). The weight fraction of inorganic ML powders approached 28.7 wt% for PMA-based composites, while in the case of PMMA- and PBMA-based composites, the amount of inorganic ML powders was 12.1 and 13.4 wt% (Table S1).

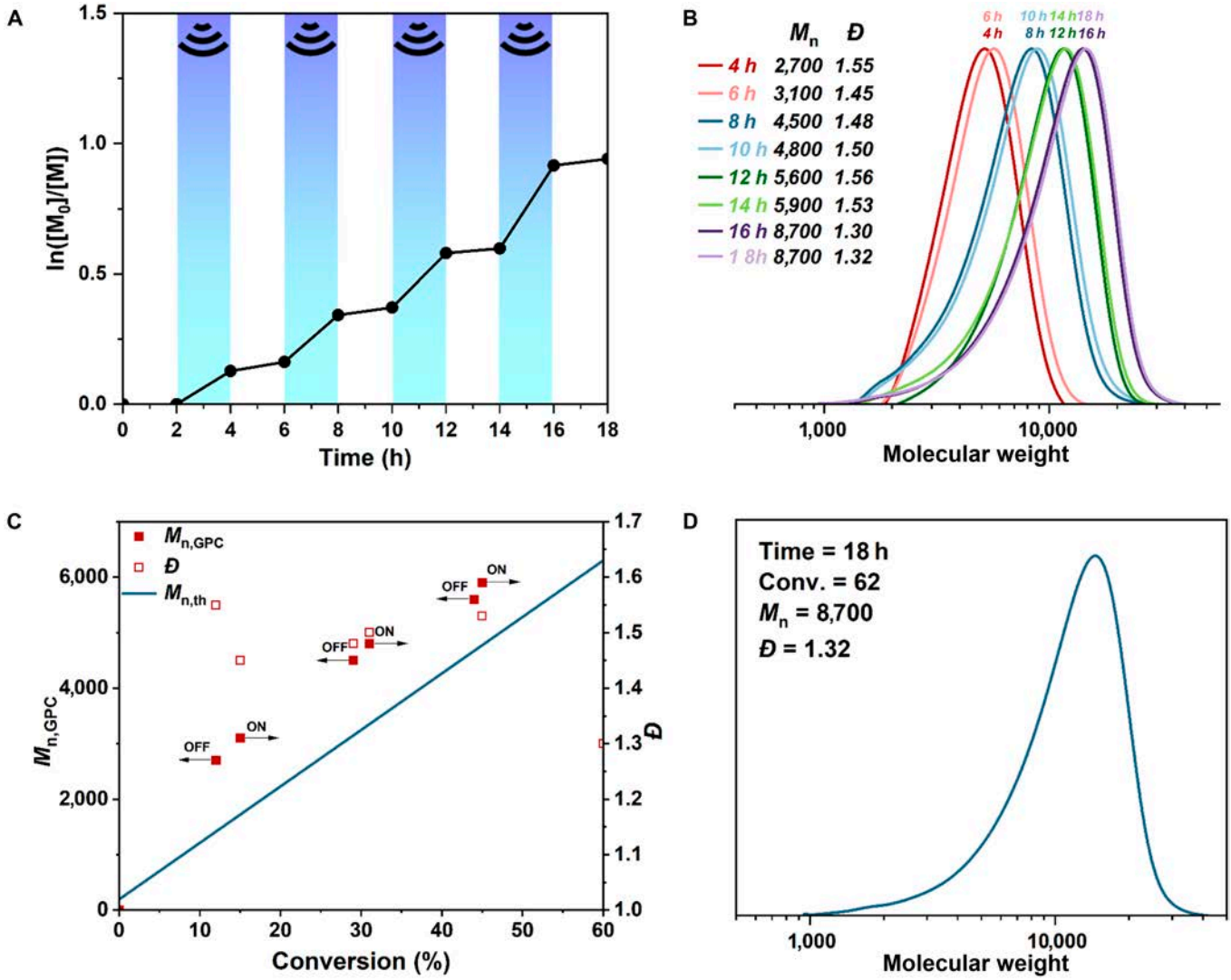


Fig. 3. (A) Temporal control in mechano-ATRP of MMA by switching US between the on/off states in the presence of the 4.8-wt% ML powders. (B) GPC analysis of the resulting polymer during 18 h ($4^1/_2$ cycles of light on/off periods). (C) Molecular weight and conversion rate, target molecular weight. (D) GPC traces of the resulting polymer after 18 h. Reaction conditions: $[MMA]_0/[CuBr_2]_0/[TPMA]_0/[EBiB]_0 = 100/0.03/0.12/1$, 50% (v/v) DMSO, 25 °C, 45 kHz, 300 W.

Discussion

In summary, the intriguingly piezoelectric and ML CaZnOS-ZnS-SrZnOS: Mn^{2+} has been demonstrated to facilitate the mechanoactivation of the ATRP process and construct mechanoresponsive polymer composites. This mechano-ATRP procedure with ML materials is compatible with a broad scope of monomers, providing well-defined polymers with high chain-end fidelity and predetermined molecular weights. In addition, the polymerization process can be temporally controlled by switching the ultrasonic bath on and off. Taking advantage of this mechano-ATRP procedure, repeatably ML polymer composites with various T_g have been successfully prepared. This work provides new sight into the design of ML polymers and lay a foundation for the development of mechano-photoresponsive polymers in the future.

Materials and Methods

Materials

ML powders, TPMA was synthesized according to previous work. Others of the chemicals were purchased from commercial sources. EBiB (99%), copper bromide ($CuBr_2$, 99%), DMSO (>99%), N, N-dimethylformamide (DMF, >99%), anisole (>99%), tetrahydrofuran (THF, ≥99.9%), 2,5-dihydroxybenzoic acid (2,5-DHB, 98%) and deuterated chloroform ($CDCl_3$, 99%) were purchased from Rhawn. MA (99%), MMA (99%), BA (98%), BMA (99%), MEMA (98%), and EA (99%) were purchased from Adamas and purified by passing through a column of basic alumina to remove inhibitors. All chemicals were used as received unless otherwise indicated.

Characterization

All the monomer conversions were performed via ^1H NMR in $CDCl_3$ using a Bruker Avance Neo 500 MHz spectrometer at 25 °C. The molecular weights and dispersity were determined using an Agilent 1260 high performance liquid chromatography system equipped with a G7110B pump and a G7162A refractive index detector. All polymers were performed in THF solution (>99.8%, high performance liquid chromatography) at 35 °C with an elution rate of 0.5 ml min^{-1}. The apparent molecular weights were determined on single photoluminescence gel

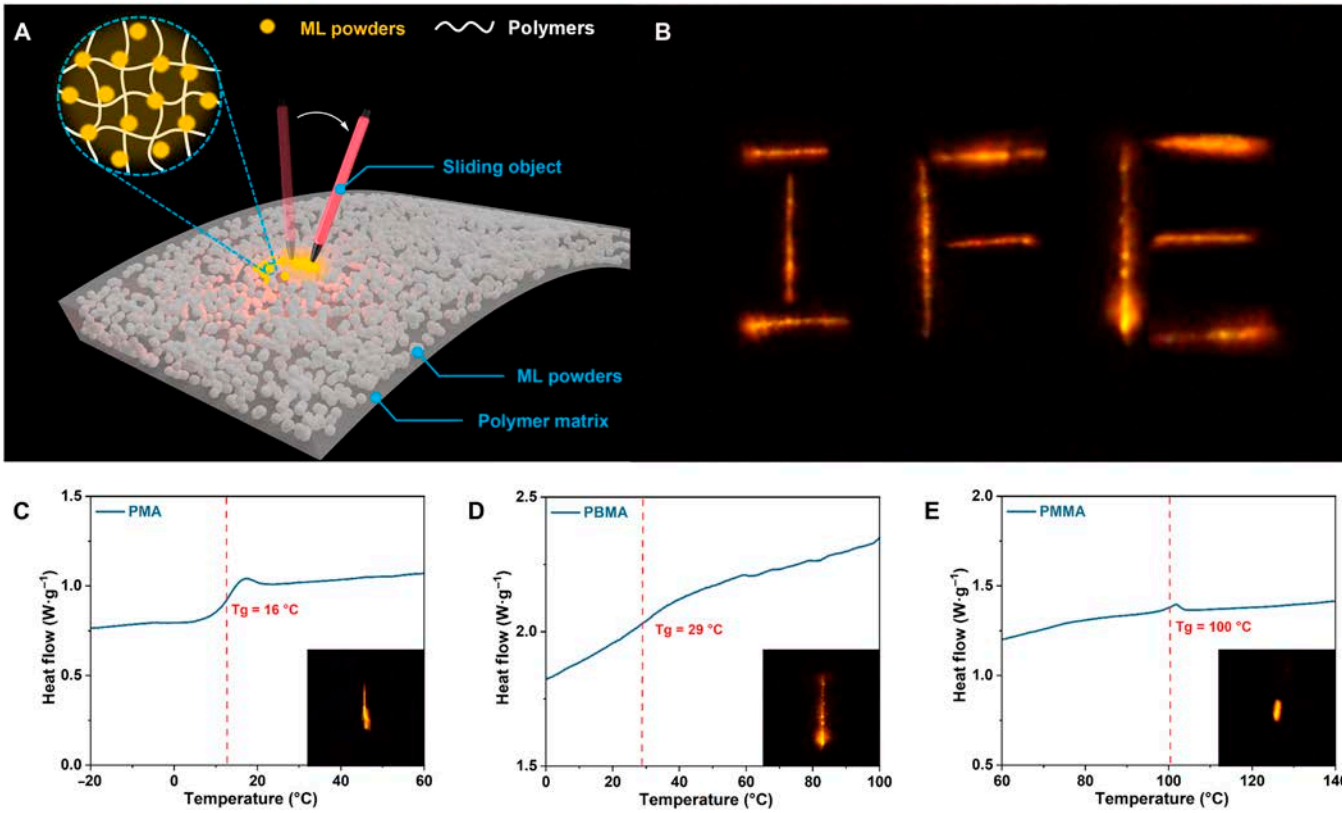


Fig. 4. (A) Structure of the ML polymer composites. (B) Superimposed image showing the complete trajectory of letters "IFE". (C to E) DSC trace of PMA-, PBMA-, and PMMA-based composites and images of mechanoluminescence triggered by scraping with a pen.

MIXED-C columns using linear poly (methyl methacrylate) standards. Prior to the analysis, the sample was diluted with THF and filtered through a column of neutral alumina to remove Cu (II) and then filtered through a 0.22-μm nylon (NY) membrane filter before injecting it into the GPC columns (injection volume: 10 μl). Mechano-induced polymerization was performed in an ultrasonic bath (KUNSHAN KQ-300VDE, 45 kHz, 300 W), and the temperature was maintained in the range of 20 to 30 °C by immersing a hollow Cu cooling coil with circulating running water in the bath. The reaction device was placed in the ultrasonic bath for 1 h, and the temperature was observed until the temperature stabilized. All the conversions were measured using ^{1}H NMR and the molecular weights were determined via GPC. The dried samples were heat pressed using an HP-100 heat-pressing machine (Hefei Kejing Material Technology Co., Ltd.) at 120 °C and 10 MPa for 10 min. The samples cooled to 25 °C spontaneously to give a hybrid material with 2-mm thickness. The ML spectra were collected from a spectrometer of Ocean Optic QE6500 with a liquid-nitrogen-cooled power detector (S7031-1006, HANANATSU). The scanning electron microscope images were obtained by a Zeiss Gemini SEM 300. The x-ray-induced luminescence patterns were obtained using an Omni-λ 300i spectrograph (Zolix) equipped with an x-ray tube (Model RACA-3, Zolix Instruments Co. Ltd., Beijing, China). The photoluminescence images were obtained using a Hitachi F-4600 spectrophotometer equipped with an R928 photomultiplier detector. MALDI-TOF mass spectrometer was from Bruke, Germany. The MALDI instrument was equipped with a 337-nm pulsed nitrogen laser (laser intensity of 50 Hz). The number of laser irradiations was 100 for all mass spectra (delay time of 190 ns), with a 20-kV acceleration voltage. MALDI experiment was carried out using 2,5-DHB as the matrix. The matrix solution was prepared by dissolving 40 mg of 2,5-DHB in 1 ml of THF. Thermogravimetric analysis measurements were performed using a TG 209 F3 (German NETZSCH) and 80-μl aluminum oxide pans. The measurements were done under nitrogen and/or oxygen (quality 5.0) atmosphere and a gas flow of 50 ml/min for both gases. The heating rates was 10 °C/min.

General procedure for ultrasonication-mediated ATRP of MA

One milliliter of MA (0.96 g, 11 mmol, 200 equiv.), 8.2 μl of EBiB (10.8 mg, 0.056 mmol, 1 equiv.), 0.72 mg of $CuBr_2$ (3.2 μmol, 0.03 equiv.), 3.7 mg of TPMA (12.9 μmol, 0.12 equiv.), 100-mg ML, and 1 ml of DMSO were added to a 10-ml Schlenk flask. The oxygen inside the flask was removed by N_2 bubbling method for 15 min and sealed. The reaction was placed in US bath for polymerization. The reaction was removed from the ultrasonic bath and exposed to air to quench the reaction.

After the reaction, samples were withdrawn from the bottle to analyze the conversion by ^{1}H NMR and number-average molecular weight (M_n) and dispersity ($Đ$) by GPC. THF (4 ml) was added to dilute a small part extracted from reaction mixture that then passed through neutral Al_2O_3 to remove catalysts. Then, 1.5 ml of sample was removed to test GPC.

Synthesis of a PMA-Br macroinitiator

Five milliliters of MA (4.8 g, 55 mmol, 200 equiv.), 41 μl of EBiB (54 mg, 0.28 mmol, 1 equiv.), 3.6 mg of $CuBr_2$ (8.5 μmol, 0.03

equiv.), 10.0 mg of TPMA (34 μmol, 0.12 equiv.) 500-mg ML, and 5 ml of DMSO were added to a 10-ml Schlenk flask. The reaction flask was sealed and degassed by N_2 purging for 15 min. The reaction was placed in US bath for polymerization. After 2 h, conversion, number-average molecular weight (M_n), and dispersity ($Đ$) were tested in the same way as described above. The macroinitiator was obtained by precipitation in mixture of cooled MeOH/H_2O (6/1, v/v) and dried under vacuum at 60 °C. Synthesized PMA-Br homopolymer could be used for subsequent chain extension reaction.

Chain extension reaction of PMA-Br with EA

One milliliter of EA (0.92 g, 9.2 mmol, 200 equiv.), 184 mg of the macroinitiator (PMA-Br, 46 μmol, 1 equiv.), 0.31 mg of CuBr2 (1.4 μmol, 0.03 equiv.), 1.6 mg of TPMA (5.5 μmol, 0.12 equiv.) 100-mg ML and 1 ml of DMSO were added to a 10-ml Schlenk flask. The oxygen inside the flask was removed by N_2 bubbling method for 15 min and sealed. The reaction was exposed to ultrasonic agitation for 4 h. Samples were withdrawn from the vial to analyze the conversion using ^{1}H NMR and the number-average molecular weight (M_n) and dispersity ($Đ$) using GPC with THF as an eluent using a linear PMMA standard.

Synthesis of ML hybrid material with BMA

Four milliliters of BMA (3.6 g, 25.2 mmol, 400 equiv.), 9.2 μl of EBiB (12.3 mg, 63.1 μmol, 1 equiv.), 0.42 mg of $CuBr_2$ (1.8 μmol, 0.03 equiv.), 2.18 mg of TPMA (7.5 μmol, 0.12 equiv.), 400-mg ML, and 4 ml of mixed solvents (DMF/anisole = 1/1) were added to a 25-ml Schlenk flask. The reaction flask was sealed and degassed by N_2 purging for 30 min. Reactions were placed in an US bath for 8 h. Then, conversion, number-average molecular weight (M_n), and dispersity ($Đ$) were tested in the same way as described above. The polymer was obtained by precipitation in mixture of cooled MeOH/H_2O (4/1, v/v) and dried under vacuum at 60 °C. The hybrid material was prepared by compression molding at 120 °C.

Synthesis of ML hybrid material with MA

Four milliliters of MA (3.8 g, 44.5 mmol, 400 equiv.), 16.3 μl of EBiB (21.7 mg, 111.2 μmol, 1 equiv.), 0.74 mg of $CuBr_2$ (3.3 μmol, 0.03 equiv.), 3.9 mg of TPMA (13.3 μmol, 0.12 equiv.), 400-mg ML, and 4 ml of DMSO were added to a 25-ml Schlenk flask. The reaction flask was sealed and degassed by N_2 purging for 30 min. Reactions were placed in an US bath for 4 h. Then, conversion, number-average molecular weight (M_n), and dispersity ($Đ$) were tested in the same way as described above. The polymer was obtained by precipitation in mixture of cooled MeOH/H_2O (3/1, v/v) and dried under vacuum at 60 °C. The hybrid material was prepared by compression molding at 130 °C.

Synthesis of ML hybrid material with MMA

Four milliliters of methyl methacrylate (MMA, 3.8 g, 37.7 mmol, 400 equiv.), 13.8 μl of EBiB (18.3 mg, 94.1 μmol, 1 equiv.), 0.63 mg of $CuBr_2$ (2.8 μmol, 0.03 equiv.), 3.3 mg of TPMA (11.3 μmol, 0.12 equiv.), 400-mg ML, and 4 ml of DMSO were added to a 25-ml Schlenk flask. The reaction flask was sealed and degassed by N_2 purging for 30 min. Reactions were placed in an US bath for 14 h. Then, conversion, number-average molecular weight (M_n), and dispersity ($Đ$) were tested in the same way as described above. The polymer was obtained by precipitation in a mixture of cooled MeOH/H_2O (2/1, v/v) and dried under vacuum at 60 °C. The hybrid material was prepared by compression molding at 150 °C.

Acknowledgments

Funding: This work was supported by the National Key Research and Development Program of China (2020YFB2008501), the National Natural Science Foundation of China (21901207), and Shaanxi Science and Technology Fund (2020JQ-137) for financial support. **Competing interests:** The authors declare that there is no conflict of interest regarding the publication of this article.

Data Availability

All data needed to evaluate the conclusions in the paper are present in the paper or the Supplementary Materials.

Supplementary Materials

Figs. S1 to S28
Table S1

References

1. Andersen J, Mack J. Mechanochemistry and organic synthesis: From mystical to practical. *Green Chem*. 2018;20(7):1435–1443.
2. Do J-L, Friščić T. Mechanochemistry: A force of synthesis. *ACS Cent Sci*. 2017;3(1):13–19.
3. Friščić T, Mottillo C, Titi HM. Mechanochemistry for synthesis. *Angew Chem Int Ed*. 2020;59(3):1018–1029.
4. Mateti S, Mathesh M, Liu Z, Tao T, Ramireddy T, Glushenkov AM, Yang W, Chen YI. Mechanochemistry: A force in disguise and conditional effects towards chemical reactions. *Chem Commun*. 2021;57:1080–1092.
5. Zeitler SM, Chakma P, Golder MR. Diaryliodonium salts facilitate metal-free mechanoredox free radical polymerizations. *Chem Sci*. 2022;13(14):4131–4138.
6. Nothling MD, Daniels JE, Vo Y, Johan I, Stenzel MH. Mechanically activated solid state radical polymerization and cross-linking via piezocatalysis. *Angew Chem Int Ed*. 2023;62(20):e202218955.
7. Brantley JN, Wiggins KM, Bielawski CW. Polymer mechanochemistry: The design and study of mechanophores. *Polym Int*. 2013;62(1):2–12.
8. Li J, Nagamani C, Moore JS. Polymer mechanochemistry: From destructive to productive. *Acc Chem Res*. 2015;48(8):2181–2190.
9. Kim G, Lau VM, Halmes AJ, Oelze ML, Moore JS, Li KC. High-intensity focused ultrasound-induced mechanochemical transduction in synthetic elastomers. *Proc Natl Acad Sci*. 2019;116(21):10214–10222.
10. Yang J, Horst M, Werby SH, Cegelski L, Burns NZ, Xia Y. Bicyclohexene-peri-naphthalenes: Scalable synthesis, diverse functionalization, efficient polymerization, and facile mechanoactivation of their polymers. *J Am Chem Soc*. 2020;142(34):14619–14626.
11. Ghanem MA, Basu A, Behrou R, Boechler N, Boydston AJ, Craig SL, Lin Y, Lynde BE, Nelson A, Shen H, et al. The role of polymer mechanochemistry in responsive materials and additive manufacturing. *Nat Rev Mater*. 2021;6(1):84–98.

12. Yang J, Xia Y. Mechanochemical generation of acid-degradable poly(enol ether)s. *Chem Sci*. 2021;12(13):4389–4394.
13. Chen Y, Mellot G, van Luijk D, Creton C, Sijbesma RP. Mechanochemical tools for polymer materials. *Chem Soc Rev*. 2021;50(6):4100–4140.
14. Chen W, Zhang H, Zhou Q, Zhou F, Zhang Q, Su J. Smart hydrogels for bone reconstruction via modulating the microenvironment. *Research*. 2023;6:0089.
15. Akbulatov S, Tian Y, Huang Z, Kucharski T, Yang Q-Z, Boulatov R. Experimentally realized mechanochemistry distinct from force-accelerated scission of loaded bonds. *Science*. 2017;357(6348):299–303.
16. Lin Y, Kouznetsova T, Craig S. A latent mechanoacid for time-stamped mechanochromism and chemical signaling in polymeric materials. *J Am Chem Soc*. 2020;142(1):99–103.
17. Chen Z, Mercer J, Zhu X, Romaniuk J, Pfattner R, Cegelski L, Martinez T, Burns N, Xia Y. Mechanochemical unzipping of insulating polyladderene to semiconducting polyacetylene. *Science*. 2017;357(6350):475–479.
18. Sun Y, Neary WJ, Burke ZP, Qian H, Zhu L, Moore JS. Mechanically triggered carbon monoxide release with turn-on aggregation-induced emission. *J Am Chem Soc*. 2022;144(3):1125–1129.
19. Wang Q, Gossweiler G, Craig S, Zhao X. Cephalopod-inspired design of electro-mechano-chemically responsive elastomers for on-demand fluorescent patterning. *Nat Commun*. 2014;5:4899.
20. Chen Y, Spiering A, Karthikeyan S, Peters G, Meijer E, Sijbesma R. Mechanically induced chemiluminescence from polymers incorporating a 1,2-dioxetane unit in the main chain. *Nat Chem*. 2012;4(7):559–562.
21. Beiermann BA, Kramer SLB, Moore JS, White SR, Sottos NR. Role of mechanophore orientation in mechanochemical reactions. *ACS Macro Lett*. 2012;1(1):163–166.
22. Robb MJ, Kim TA, Halmes AJ, White SR, Sottos NR, Moore JS. Regioisomer-specific mechanochromism of naphthopyran in polymeric materials. *J Am Chem Soc*. 2016;138(38):12328–12331.
23. Davis D, Hamilton A, Yang J, Cremar L, Gough D, Potisek S, Ong M, Braun P, Martinez T, White S, et al. Force-induced activation of covalent bonds in mechanoresponsive polymeric materials. *Nature*. 2009;459(7243):68–72.
24. Zhang H, Chen Y, Lin Y, Fang X, Xu Y, Ruan Y, Weng W. Spiropyran as a mechanochromic probe in dual cross-linked elastomers. *Macromolecules*. 2014;47(19):6783–6790.
25. Wu M, Li Y, Yuan W, De Bo G, Cao Y, Chen Y. Cooperative and geometry-dependent mechanochromic reactivity through aromatic fusion of two rhodamines in polymers. *J Am Chem Soc*. 2022;144(37):17120–17128.
26. Potisek SL, Davis DA, Sottos NR, White SR, Moore JS. Mechanophore-linked addition polymers. *J Am Chem Soc*. 2007;129(45):13808–13809.
27. Larsen MB, Boydston AJ. Successive Mechanochemical activation and small molecule release in an elastomeric material. *J Am Chem Soc*. 2014;136(4):1276–1279.
28. Verstraeten F, Göstl R, Sijbesma RP. Stress-induced colouration and crosslinking of polymeric materials by mechanochemical formation of triphenylimidazolyl radicals. *Chem Commun*. 2016;52(55):8608–8611.
29. Di Giannantonio M, Ayer MA, Verde-Sesto E, Lattuada M, Weder C, Fromm KM. Triggered metal ion release and oxidation: Ferrocene as a Mechanophore in polymers. *Angew Chem Int Ed*. 2018;57(35):11445–11450.
30. Stratigaki M, Göstl R. Methods for exerting and sensing force in polymer materials using mechanophores. *ChemPlusChem*. 2020;85(6):1095–1103.
31. He W, Yuan Y, Wu M, Li X, Shen Y, Qu Z, Chen Y. Multicolor chromism from a single chromophore through synergistic coupling of mechanochromic and photochromic subunits. *Angew Chem Int Ed*. 2023;62(11):e202218785.
32. Kim G, Wu Q, Chu JL, Smith EJ, Oelze ML, Moore JS, Li KC. Ultrasound controlled mechanophore activation in hydrogels for cancer therapy. *Proc Natl Acad Sci*. 2022;119(4):e2109791119.
33. Zhou Y-N, Li J-J, Wu Y-Y, Luo Z-H. Role of external field in polymerization: Mechanism and kinetics. *Chem Rev*. 2020;120(5):2950–3048.
34. Bian C, Li S, Yang N, Chen H, Feng W, Zhou Y-N, Luo Z-H. In-depth mechanistic and kinetic investigation of sonochemically mediated atom transfer radical polymerization using modeling approach. *Chem Eng J*. 2023;464:142642.
35. Kapil K, Szczepaniak G, Martinez MR, Murata H, Jazani AM, Jeong J, Das SR, Matyjaszewski K. Visible-light-mediated controlled radical branching polymerization in water. *Angew Chem Int Ed*. 2023;62(10):e202217658.
36. Lorandi F, Fantin M, Matyjaszewski K. Atom transfer radical polymerization: A mechanistic perspective. *J Am Chem Soc*. 2022;144(34):15413–15430.
37. Ayarza J, Wang Z, Wang J, Huang C-W, Esser-Kahn AP. 100th anniversary of macromolecular science viewpoint: Piezoelectrically mediated mechanochemical reactions for adaptive materials. *ACS Macro Lett*. 2020;9(9):1237–1248.
38. Ren Z, Peng Y, He H, Ding C, Wang J, Wang Z, Zhang Z. Piezoelectrically mediated reactions: From catalytic reactions to organic transformations. *Chin J Chem*. 2023;41(1):111–128.
39. Parnitzke B, Nwoko T, Bradford KGE, De Alwis Watuthanthrige N, Yehl K, Boyer C, Konkolewicz D. Photons and photocatalysts as limiting reagents for PET-RAFT photopolymerization. *Chem Eng J*. 2023;456:141007.
40. Bobrin VA, Zhang J, Corrigan N, Boyer C. The emergence of reversible–deactivation radical polymerization in 3D printing. *Adv Mater Technol*. 2023;8:20.
41. Sifri RJ, Kennedy AJ, Fors BP. Photocontrolled cationic degenerate chain transfer polymerizations via thioacetal initiators. *Polym Chem*. 2020;11:6499–6504.
42. Rosenbloom SI, Sifri RJ, Fors BP. Achieving molecular weight distribution shape control and broad dispersities using RAFT polymerizations. *Polym Chem*. 2021;12(34):4910–4915.
43. Mohapatra H, Kleiman M, Esser-Kahn AP. Mechanically controlled radical polymerization initiated by ultrasound. *Nat Chem*. 2017;9:135–139.
44. Wang Z, Pan X, Li L, Fantin M, Yan J, Wang Z, Wang Z, Xia H, Matyjaszewski K. Enhancing mechanically induced ATRP by promoting interfacial electron transfer from piezoelectric nanoparticles to cu catalysts. *Macromolecules*. 2017;50(20):7940–7948.
45. Wang Z, Pan X, Yan J, Dadashi-Silab S, Xie G, Zhang J, Wang Z, Xia H, Matyjaszewski K. Temporal control in mechanically controlled atom transfer radical polymerization using low ppm of cu catalyst. *ACS Macro Lett*. 2017;6(5):546–549.
46. Zhou Y-N, Li J-J, Ljubic D, Luo Z-H, Zhu S. Mechanically mediated atom transfer radical polymerization: Exploring its potential at high conversions. *Macromolecules*. 2018;51(17):6911–6921.

47. Xu S, Zhang W, Wang C, Peng W, Shi G, Cui Z, Fu P, Liu M, He Y, Qiao X, et al. Mechanically induced atom transfer radical polymerization with high efficiency via piezoelectric heterostructures. *Polymer*. 2022;252:124949.
48. Ding C, Yan Y, Peng Y, Wu D, Shen H, Zhang J, Wang Z, Zhang Z. Piezoelectrically mediated reversible addition–fragmentation chain-transfer polymerization. *Macromolecules*. 2022;55(10):4056–4063.
49. Liu K, Zhang W, Zong L, He Y, Zhang X, Liu M, Shi G, Qiao X, Pang X. Dimensional optimization for ZnO-based mechano-ATRP with extraordinary activity. *J Phys Chem Lett*. 2022;13(22):4884–4890.
50. Zhou M, Zhang Y, Shi G, He Y, Cui Z, Zhang X, Fu P, Liu M, Qiao X, Pang X. Mechanically driven atom transfer radical polymerization by piezoelectricity. *ACS Macro Lett*. 2023;12(1):26–32.
51. Chakma P, Zeitler SM, Baum F, Yu J, Shindy W, Pozzo LD, Golder MR. Mechanoredox catalysis enables a sustainable and versatile reversible addition-fragmentation chain transfer polymerization process. *Angew Chem Int Ed*. 2023;62:e202215733.
52. Zhang Z, Liu C, Li C, Wu W, Jiang X. Shape effects of cylindrical versus spherical unimolecular polymer nanomaterials on in vitro and in vivo behaviors. *Research*. 2019;2019:2391486.
53. Cheng L, Wang Y, Sun G, Wen S, Deng L, Zhang H, Cui W. Hydration-enhanced lubricating electrospun nanofibrous membranes prevent tissue adhesion. *Research*. 2020;2020:4907185.
54. Zhao X, Sun C, Xiong F, Wang T, Li S, Huo F, Yao X. Polymerization-induced self-assembly for efficient fabrication of biomedical nanoplatforms. *Research*. 2023;6:0113.
55. Mohapatra H, Ayarza J, Sanders EC, Scheuermann AM, Griffin PJ, Esser-Kahn AP. Ultrasound promoted step-growth polymerization and polymer crosslinking via copper catalyzed azide–alkyne "click" reaction. *Angew Chem Int Ed*. 2018;57(35):11208–11212.
56. Wang Z, Ayarza J, Esser-Kahn AP. Mechanically initiated bulk-scale free-radical polymerization. *Angew Chem Int Ed*. 2019;58(35):12023–12026.
57. Ayarza J, Wang Z, Wang J, Esser-Kahn A. Mechanically promoted synthesis of polymer organogels via disulfide bond cross-linking. *ACS Macro Lett*. 2021;10(7):799–804.
58. Wang Z, Wang J, Ayarza J, Steeves T, Hu Z, Manna S, Esser-Kahn AP. Bio-inspired mechanically adaptive materials through vibration-induced crosslinking. *Nat Mater*. 2021;20(6):869–874.
59. Tsarevsky NV, Matyjaszewski K. Reversible redox cleavage/coupling of polystyrene with disulfide or thiol groups prepared by atom transfer radical polymerization. *Macromolecules*. 2002;35:9009–9014.
60. Wu L, Cio S, Azevedo H, Gautrot J. Photo-configurable, cell-remodelable disulfide crosslinked hyaluronic acid hydrogels. *Biomacromolecules*. 2020;21(12):4663–4672.
61. Xu H, Shi J-L, Lyu S, Lang X. Visible-light photocatalytic selective aerobic oxidation of thiols to disulfides on anatase TiO_2. *Chin J Catal*. 2020;41:1468–1473.
62. Peng D, Jiang Y, Huang B, Du Y, Zhao J, Zhang X, Ma R, Golovynskyi S, Chen B, Wang F. A ZnS/CaZnOS heterojunction for efficient mechanical-to-optical energy conversion by conduction band offset. *Adv Mater*. 2020;32(16):1907747.
63. Jia J, Fu L, Gao X, Dong S, Xu Y, Wang D, Zou G. Ternary-host and heterojunction enabled eye-visible elastic mechanoluminescence from $(Ca_{0.5}Sr_{0.5})ZnOS/xZnS/Mn^{2+}$. *J Phys Chem C*. 2022;126(3):1523–1530.
64. Wang C, Ma R, Peng D, Liu X, Li J, Jin B, Shan A, Fu Y, Dong L, Gao W, et al. Mechanoluminescent hybrids from a natural resource for energy-related applications. *InfoMat*. 2021;3(1):1272–1284.
65. Li X, Wang C, Zheng Y, Huang Z, Luo J, Zhu M, Liang T, Ren B, Zhang X, Wang D, et al. Smart semiconductor-heterojunctions mechanoluminescence for printable and wearable sports light sources. *Mater Des*. 2023;225:111589.
66. Li W, Cai Y, Chang J, Wang S, Liu J, Zhou L, Wu M, Zhang J-C. Unraveling mechanoluminescent mechanisms in doped CaZnOS materials: Co-mediation of trap-controlled and non-trap-controlled processes. *Adv Funct Mater*. 2023;2305482.
67. Murray KK, Boyd RK, Eberlin MN, Langley GJ, Li L, Maito Y. Definitions of terms relating to mass spectrometry. *Pure Appl Chem*. 2013;85(7):1515–1609.
68. Wyzgoski FJ, Polce MJ, Wesdemiotis C, Arnould MA. Matrix-assisted laser desorption/ionization time-of-flight mass spectrometry investigations of polystyrene and poly (methyl methacrylate) produced by monoacylphosphine oxide photoinitiation. *J Polym Sci A Polym Chem*. 2007;45(11):2161–2171.